Received: 19 March 2018 | Accepted: 27 March 2018

DOI: 10.1111/ijac.12904

International Journal of Applied Ceramic Technology

ORIGINAL ARTICLE

Processing, structural, and biological evaluations of zirconia scaffolds coated by fluorapatite

Beltina León[1] | **María Albano**[1] | **Liliana Garrido**[1] | **Emanuela Ferraz**[2] | **Adalberto Rosa**[2] | **Paulo Tambasco de Oliveira**[2]

[1]CCT-La Plata CONICET, CICPBA, Centro de Tecnología de Recursos Minerales y Cerámica (CETMIC), Provincia de Buenos Aires, Argentina

[2]School of Dentistry of Ribeirão Preto, University of São Paulo (FORP-USP), Ribeirão Preto, São Paulo, Brazil

Correspondence
María Albano
Email: palbano@cetmic.unlp.edu.ar

Funding information
Fundação de Amparo à Pesquisa do Estado de São Paulo, Grant/Award Number: 2012/50949-4; Consejo Nacional de Investigaciones Científicas y Técnicas, Grant/Award Number: PIP 0454

Abstract

Highly porous zirconia (ZrO_2) scaffolds fabricated by the replication method were coated with fluorapatite (FA). The FA coating was obtained by dipping the ZrO_2 scaffolds into stabilized aqueous FA slips having different viscosity values (≤5.0 mPa.s). The influence of the FA slip viscosity and the immersion time on the reduction in the scaffold porosity and microstructure of the coated scaffolds were investigated. Cell spreading and survival of bone marrow-derived stromal cells (BMSC) and pre-osteoblastic MC3T3-E1 cells on the uncoated and coated scaffolds were examined using fluorescence and SEM microscopy, and MTT assay.The FA slip with the lowest viscosity value did not lead to a continuous film along the strut network and the macropores remained uncoated. The slips with the highest viscosity value produced a partial blocking of macropores. The porous structure obtained after coating with slips of 2.2 mPa.s viscosity for 2 seconds exhibited a low reduction in porosity and pore size (400-420 μm), due to the formation of the FA layer, and a continuous film distributed along the strut surfaces. Morphology, spreading, and survival of BMSC and MC3T3-E1 cells over a 7-day culture period evidenced good biocompatibility of FA-coated ZrO_2 scaffolds processed by dip coating.

KEYWORDS

cell viability, fluorapatite dip coating, fluorapatite slip viscosity, scaffold porous structures, ZrO_2 scaffolds

1 | INTRODUCTION

Calcium orthophosphates ceramics, such as fluorapatite ($Ca_{10}(PO_4)_6F_2$), have attracted a great deal of attention in orthopedic applications and in dentistry surgeries.[1,2] In a review paper, Dorozhkin et al[3] explained that fluorapatite is biocompatible, exhibits bioactive behavior and integrates into living tissue; these characteristics lead to an intimate physicochemical bond between the implants and bone, termed osseointegration. However, Suchanek and Yoshimura[4] demonstrated that the poor mechanical properties of fluorapatite, such as low strength and fracture toughness, limited its application in form of highly porous scaffolds, eg for bone tissue engineering applications, making very difficult their handling during surgical procedures and facing a high probability of failure after implantation. In biomedical applications FA is used primarily as fillers and coatings. FA as a coating material has been reported[5,6] to have lower solubility relative to hydroxyapatite; the decrease in solubility of FA films can improve their lifetime or stability in vivo.

On the other hand, Kelly and Denry[7] described that 3 mol% yttria-partially stabilized zirconia is used as a structural ceramic due to its excellent mechanical

properties; and Piconi and Maccauro[8] showed that it can be used as a ceramic biomaterial. In this study, a porous ZrO_2 scaffold was chosen as a framework and the fluorapatite was used as a coating layer; the idea behind this approach was to combine the bioactivity of FA with the mechanical benefits of ZrO_2, in order to produce a strong and bioactive porous scaffold. Chen et al[9] revealed that the production of a highly porous coated ZrO_2 scaffold was one of the crucial requirements in order to ensure exchange of ions between the scaffold and the surrounding biological environment, migration of cells and tissue formation. The FA coating was achieved by infiltrating the ZrO_2 scaffolds with an aqueous well-stabilized FA slip with poly(vinyl) alcohol (PVA).

In order to achieve a continuous thin film of fluorapatite uniformly distributed along the strut surfaces and inside the macropores of the ZrO_2 scaffold, the rheological behaviour and viscosity of aqueous FA slips should be investigated. Relatively low slip viscosity can only be achieved in the presence of an optimum dispersion state of particles. Ammonium polyacrylate (NH_4PA) is an anionic polyelectrolyte commonly used as dispersant of ceramic powders in aqueous media as described by Cesarano and Aksay.[10] Guldberg-Pedersen and Bergstrom[11]demonstrated that the polyelectrolyte adsorbs at the solid-liquid interface and enhances repulsive interactions (electrostatic and steric) between the particles. The binder such as PVA provides strong adhesion between the coating and the substrate, preventing the FA powder from detaching off the substrate during thermal treatment.

In this study, porous ZrO_2 scaffolds fabricated by the replication method were dip coated into FA aqueous slips stabilized with NH_4PA having different viscosity values. The influence of the FA slip viscosity and the immersion time on the reduction in the scaffold porosity and microstructure of the coated scaffolds were investigated. The pore size distributions of uncoated and coated ZrO_2 scaffolds produced using different dip coating slips and immersion times were compared. Since functionalized ZrO_2 scaffolds have been considered as potential bone substitutes in therapeutic strategies for bone repair,[12-14] the cell interaction with the ZrO_2 scaffold structures was evaluated in terms of cell spreading and survival in short-term bone-derived cell cultures using 2 different cell sources.

2 | EXPERIMENTAL PROCEDURES

2.1 | Raw materials and processing

A commercial 3 mol% yttria- partially stabilized zirconia (Saint-Gobain ZirPro, China, d_{50} = 0.64 μm) was used to produce the scaffolds. The scaffolds were fabricated by immersing commercial polyurethane foams (discs of 12 mm in diameter and 3 mm in thickness) in aqueous zirconia suspensions. The ZrO_2 suspensions with a solid loading in the range 35-44 wt% were obtained by dispersing ZrO_2 powder in water containing 0.11 wt% NH_4PA (Duramax D 3500; Rohm & Haas) as dispersant using an ultrasonic bath. Subsequent to this, 6 wt% PVA (degree of hydrolysis = 87%-89% and average molecular weight in the range of 57 000-66 000 g/mol) as a binder was added to the slurry, followed by additional stirring. The pH of the suspensions was adjusted to 9.0 with a diluted ammonia aqueous solution. Discs of polyurethane foams were immersed in the ZrO_2 slurry and centrifuged for 5 minutes at 250 *g*. Afterward, they were manually extracted from the ZrO_2 suspension and subsequently blown with compressed air to eliminate the excess slurry. The ZrO_2 sponges were then dried at 100°C for 24 hours. The obtained bodies were heated to burn out the sponge and binder at 800°C for 5 hours at a heating rate of 1°C/min; finally the ZrO_2 scaffolds were obtained after sintering at 1500°C for 2 hours.

The fluorapatite powder used for coating was prepared from a mixture of $Ca_3(PO_4)_2$ (Fluka, Germany) and CaF_2 (Sigma-Aldrich, Ireland) powders; these powders were mixed in a 3:1.5 ratio; thus, CaF_2 was in excess with respect to the stoichiometric ratio for the reaction:

$$3Ca_3(PO_4)_2 + CaF_2 \rightarrow Ca_{10}(PO_4)_6F_2 \quad (1)$$

The mixture of powders was calcined 3 hours at 1000°C. Then, the milling of FA powder was carried out in an attrition mill, washed with distilled water and dried at 100°C. The FA suspensions for dip coating were prepared at solid concentrations of 5, 10 and 20 wt% with 0.6 wt% NH_4PA and 5 wt% PVA. The obtained ZrO_2 scaffolds were immersed in the FA slurries for different times, then manually withdrawn from the suspension at a constant velocity and dried at 100°C for 24 hours. The FA coated ZrO_2 scaffolds were sintered at 1100°C for 2 hours.

2.2 | Characterization techniques

Steady state flow curves of FA slips were performed by measuring the steady shear stress value as a function of shear rate in the range of 0.5-542 s^{-1} using a concentric cylinder viscometer (Haake VT550, Germany) and a sensor system NV at 25°C. As soon as stationary conditions were reached at each shear rate, the shear rate increased in steps up to the maximum value and then decreased.

The density of the scaffolds (ρ_s) was determined from the dimensions and mass of the sintered bodies. The total porosity (*P*) was then calculated by:

$$P = \left(1 - \frac{\rho_s}{\rho_z}\right) \times 100 \quad (2)$$

where $\rho_z = 6.05$ g/cm^3 is the theoretical density of ZrO_2.

The total porosity of coated samples (Pc) was calculated by the modified (2) equation:

$$Pc = \left(1 - \frac{\rho_s}{\rho_z} - \frac{v_{cm}}{v_s}\right) \times 100 \quad (3)$$

where v_s is the scaffold′s volume, v_{cm} is the coating volume calculated for each sampleas:

$$v_{cm} = \frac{w_f - w_i}{\rho_{cm}} = \frac{w_f - w_i}{\rho_{FA}} \quad (4)$$

w_i and w_f are, respectively, the weight of the scaffold before and after coating. The XRD patterns of FA corresponded to JCPDS 15-0876; the coating density (ρ_{cm}) is assumed equal to 3.2 g/cm^3 which is the theoretical density of FA from JCPDS 15-0876.

The microstructure of the scaffolds was characterized using scanning electron microscopy (SEM; JEOL, JCM-6000). A quantitative assessment of pores size and struts thickness distribution was carried out by means of SEM; in order to perform a reliable statistical sampling more than 250 voids were measured from different images. The coated scaffolds were polished (with a series of diamond pastes down to 1 μm) for microstructural observation by means of SEM.

2.3 | Biological assays

Previous to cell culture experiments, the scaffolds were sterilized in dry heat at 180°C for 2 hours and then placed in 24-well polystyrene cell culture plates, one scaffold per well.

2.3.1 | Osteogenic cell cultures

The biological evaluations were performed using 2 cell cultures, one derived from a cell line and the other one from a primary culture. The mouse pre-osteoblastic cell line MC3T3-E1 subclone 14 (American Type Culture Collection, VA) was cultivated in growth media (GM) constituted by α-MEM (alpha-minimum essential medium; Invitrogen-Life Technologies, NY) supplemented with 10% bovine fetal serum (Gibco, NY), 50 μg/mL gentamicin (Gibco) and 0.3 μg/mL fungisone (Gibco). Primary rat bone marrow-derived stromal cells (BMSC) were obtained as described by Maniatopoulos et al[15] under the guidance of the Ethics Committee on Animal Use of the University of São Paulo at Ribeirão Preto (Protocol Number 2015.1.1136.58.1), and cultured in GM. After subconfluence, cultures were harvested with 1 mmol/L ethylenediamine tetra acetic acid (EDTA; Gibco) and 0.25% trypsin (Gibco). Subcultured cells were then plated in 24-well culture plates at a cell density of 2×10^4 cells per ZrO_2 scaffold and cultured in osteogenic medium (OM), which was GM supplemented with 5 μg/mL ascorbic acid (Gibco) and 7 mmol/L β-glycerophosphate (Sigma-Aldrich, MO) for periods of up to 7 days. Cultures were kept at 37°C, in a humidified atmosphere containing 5% CO_2 and 95% air; the medium was changed every 48 hours.

2.3.2 | Cell morphology by direct fluorescence microscopy and scanning electron microscopy

At 2 days of culture, MC3T3-E1 cell morphology was evaluated by direct fluorescence to detect the actin cytoskeleton and cell nuclei and by SEM as described in Albano et al[16] and Pereira et al.[17] Briefly, cells were fixed for 10 minutes at RT using 4% paraformaldehyde in 0.1 mol/L sodium phosphate buffer (PB), pH 7.2, and permeabilized with 0.5% Triton X-100 in PB for 10 minutes. Then cells were processed for fluorescence labelling using Alexa Fluor 594 (red fluorescence)-conjugated phalloidin (1:200; Molecular Probes, OR), to identify the actin cytoskeleton, and 300 nmol/L 40,6-diamidino-2-phenylindole, dihydrochloride (DAPI, Molecular Probes) to label the cell nuclei. The samples were examined under epifluorescence, using a Zeiss AxioImager M2 microscope (Carl Zeiss, Germany) outfitted with an Axio Cam MRm digital camera (Carl Zeiss). For SEM analysis, MC3T3-E1 cells were fixed for 1 hour in cacodylate buffered 2% glutaraldehyde, dehydrated to the critical point and sputter coated with gold before being viewed at 25 kV in a JEOL JSM-6610 microscope in high vacuum. The digital images were processed using Adobe Photoshop CS5.1 software (Adobe Systems, CA).

2.3.3 | MTT assay

Cell viability was assessed by 3-[4,5-dimethylthiazol-2-yl]-2,5-diphenyl tetrazolium bromide (MTT; Sigma-Aldrich) assay. At day 7 of culture, MC3T3-E1 and BMSC cultures were incubated with 10% MTT (5 mg/mL) in culture medium at 37°C for 4 hours. For qualitative analysis of the formazan-stained cells, the samples were examined under epi-illumination using a Leica MZ6 stereomicroscope (Leica Microsystems, Germany) outfitted with a Leica DFC310 FX digital camera (Leica Microsystems). The digital images were processed with Adobe Photoshop CS5.1 software (Adobe Systems). For quantitative analysis, 1 mL

acid-isopropanol (0.04 N HCl in isopropanol) was added to each well, and the solution was transferred to a 96-well plate (Corning). The optical density was read at 570-650 nm on the plate reader (μQuanti, BioTek Instruments, VT), and data were expressed as absorbance normalized to the scaffold weight (g).

2.3.4 | Statistical analysis

The data were expressed as mean ± SD and analyzed by the parametric t-test using the Sigma Plot software (Systat Software, San Jose, CA). For all comparisons, the level of significance (P) was set at .05.

3 | RESULTS

3.1 | Rheological properties and scaffold structures

The milling of the FA powder reduced the mean particle size from 3.67 to 0.37 μm. We have previously determined[18] the chemical composition of the FA powder before and after attrition milling. The chemical composition of the powder before milling indicated an excess of Ca and F with respect to the theoretical composition of $Ca_{10}(PO_4)_6F_2$. This was attributed to the excess of CaF_2, relative to the stoichiometric ratio, used in the preparation of fluorapatite (section 2.1). Ca and F were removed during the milling and washing of the powder, leading to an apatite with a Ca/P atomic ratio and a F content of 1.67 and 37 700 ppm, respectively, which were close to the theoretical one.

Figure 1A, B shows the flow curves of shear stress vs shear rate and viscosity vs shear rate, respectively, for FA slips with different solid loading at pH 9. The suspensions exhibited a nearly Newtonian behavior, well-stabilized FA slips with low viscosity values were obtained for all the solid loading. The slip viscosity markedly increased with increasing the solid content; at solid loading of 5 wt% the FA slip had the lowest viscosity value; as the FA content increased from 10 to 20 wt% the viscosity of the slips increased from 2.2 to 5.0 mPa.s, respectively.

Table 1 shows the total porosity of ZrO_2 scaffolds for different aqueous ZrO_2 slip concentrations. The porosity of the scaffolds decreased from 93% to 80% with increasing the ZrO_2 slip concentration from 35 to 44 wt%, respectively. When the porosity of the ZrO_2 scaffold was 80% some pores were partly blocked; on the other hand, the scaffolds with 93% porosity were fragile to be handle. Therefore, the scaffolds with 87% porosity were selected to be coated with a fluorapatite surface layer.

Figure 2A shows a SEM image of the ZrO_2 scaffold with 87% porosity. Figure 2B-D show SEM images of

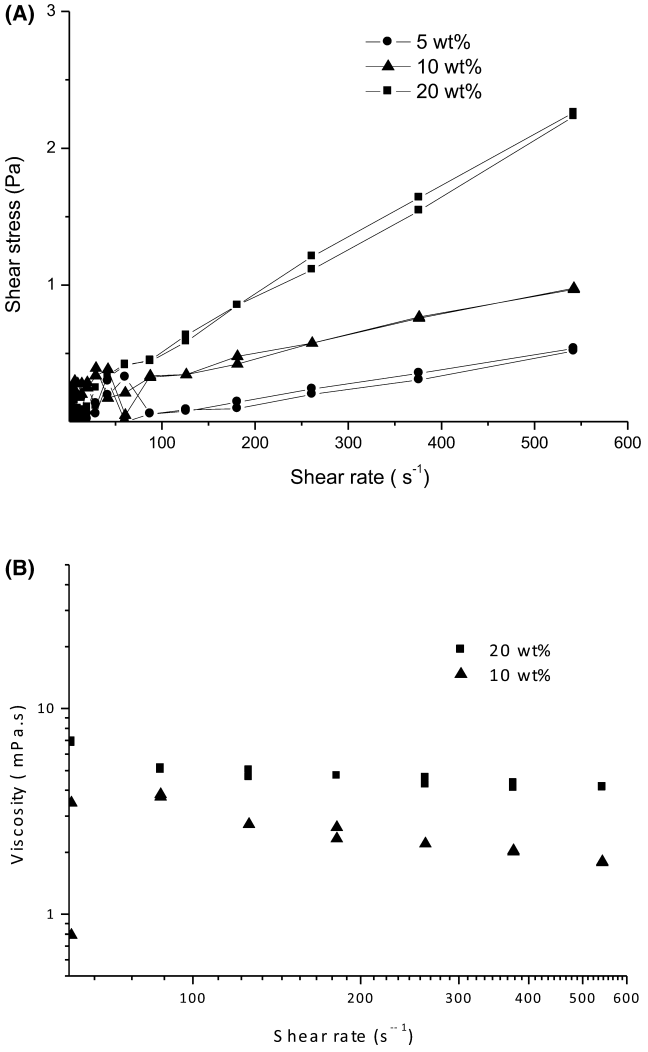

FIGURE 1 Flow curves of shear stress vs shear rate (A) and viscosity vs shear rate (B), for FA slips with 0.6 wt% NH_4PA, 5 wt% PVA with different solid loading at pH 9

TABLE 1 Total porosity of ZrO_2 scaffolds for different ZrO_2 slip concentrations

ZrO_2 slip concentration (wt%)	Total porosity (%)
35	93
40	87
44	80

the ZrO_2 scaffolds after coating with FA slips having the lowest viscosity (about 1.2 mPa.s), 2.2 and 5.0 mPa.s, respectively, for 2 seconds SEM images of the scaffolds coated with slips of 2.2 and 5.0 mPa.s for 10 seconds are, respectively, shown in Figure 2E, F. The microstructure of the coated scaffolds showed the ZrO_2 strut surface (bright phase), the FA coating (gray phase), and the pores (dark phase). SEM observations carried out on polished coated scaffolds (Figure 3)

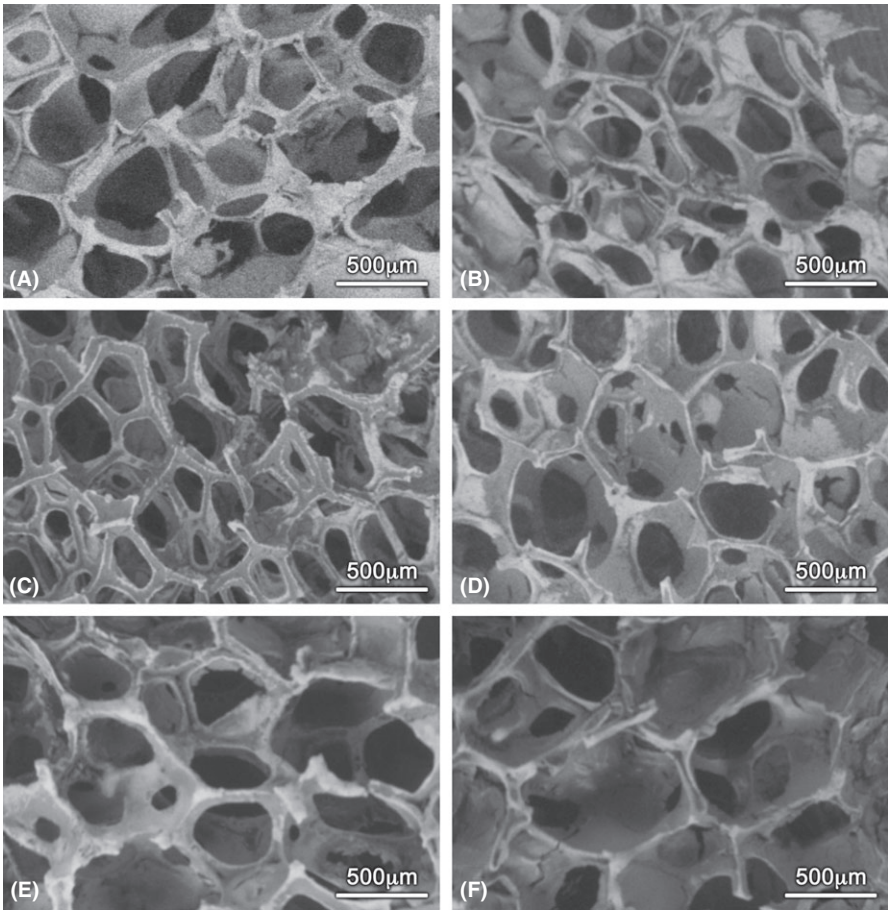

FIGURE 2 SEM images of different ZrO_2 scaffolds: uncoated (A); after coating with different FA slips and immersion times: 1.2 mPa.s for 2 s. (B), 2.2 mPa.s for 2 s. (C), 5.0 mPa.s for 2 s. (D), 2.2 mPa.s for 10 s. (E), 5.0 mPa.s for 10 s. (F). ZrO_2 (bright phase), FA coating (gray phase), pores (dark phase)

provided insights about the thickness of the FA coating layer.

Figure 4 shows the volume percent of the scaffold porosity occupied by FA and the amount of FA introduced into the scaffold per cm^3 after immersion for 2 seconds, as a function of the slip viscosity. Both, the vol% of FA and the mg FA/cm^3 introduced into the ZrO_2 scaffolds, linearly increased with increasing the slip viscosity. A low amount of FA (2.7 mg FA/cm^3) was incorporated into the scaffold after coating with slips having the lowest viscosity, resulting in a negligible reduction in the scaffold total porosity. As the dip coating slip viscosity increased to 2.2 and 5.0 mPa.s, a greater amount of FA was introduced per cm^3 and the volume percent of the scaffold porosity occupied by FA increased. Nearly 3 vol% of the scaffold porosity was occupied by FA after coating with slips of 5.0 mPa.s viscosity, in comparison with 1 vol% in the scaffolds coated with slips having a viscosity value of 2.2 mPa.s (Figure 4).

Figure 5A, B shows the pore size and strut thickness distributions, respectively, of the ZrO_2 scaffolds before and after coating with slips of different viscosities for 2 seconds. A wide pore size distribution with pore sizes between 250 and 700 μm was found for uncoated ZrO_2 scaffolds; most of the pores had sizes between 340 and 540 μm and the most frequent pore size was in the range 400-420 μm.

For the scaffolds coated with FA slips having the lowest viscosity value, a similar pore size distribution with respect to the uncoated ZrO_2 scaffold was found (Figure 5A); besides, nearly the same strut thickness distribution was observed for the uncoated and coated ZrO_2 scaffolds (Figure 5B).The struts of the uncoated and coated scaffolds with the lowest viscosity slip had thickness between 40 and 75 μm and the more frequent strut thickness was in the range 55-60 μm. The coating of the ZrO_2 scaffolds with slips of 2.2 mPa.s viscosity produced a slightly displacement of the more frequent pore size from 400-420 to 360-380 μm (Figure 5A). In addition, a scarcely increased in the most frequent strut thickness from 55-60 to 60-65 μm was measured (Figure 5B). In contrast, the pore size distribution of the ZrO_2 scaffold was significantly shifted to lower sizes after the coating with slips of 5.0 mPa.s viscosity. A strong reduction in the most frequent pore size from 400-420 to 240-260 μm (Figure 5A) occurred in accordance with the greater volume percent of the porosity occupied by FA (Figure 4). The strut thickness distribution was also shifted to significantly greater values after the coating; the most frequent strut thickness increased from 55-60 to 70-75 μm for

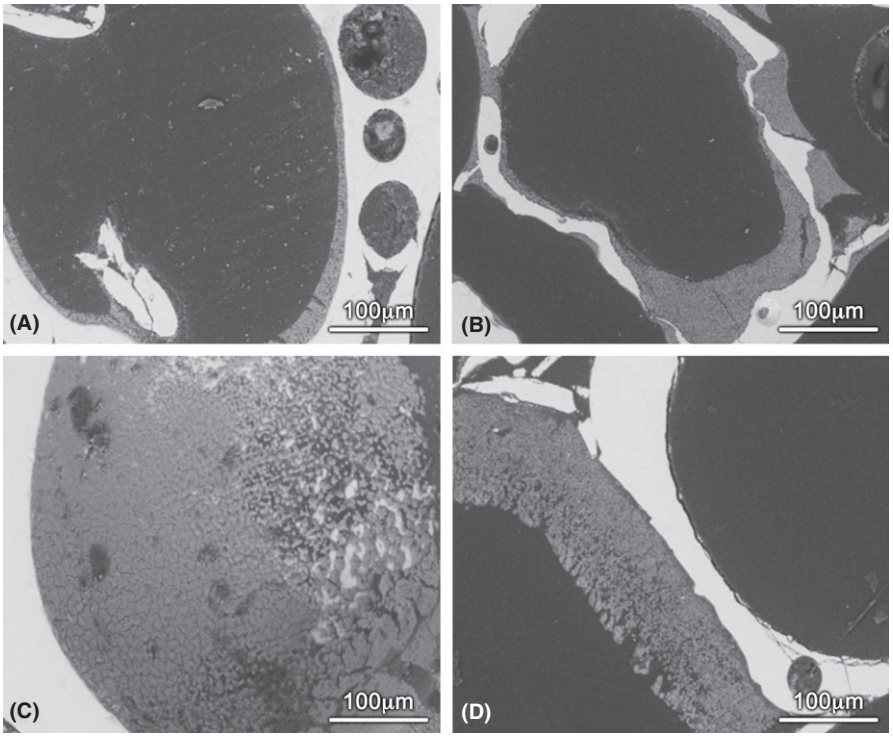

FIGURE 3 SEM images of polished scaffolds after coating with different FA slips and immersion times: 2.2 mPa.s for 2 s. (A), 5.0 mPa.s for 2 s. (B), 5.0 mPa.s for 10 s. (C,D). ZrO_2 (bright phase), FA coating (gray phase), pores (dark phase)

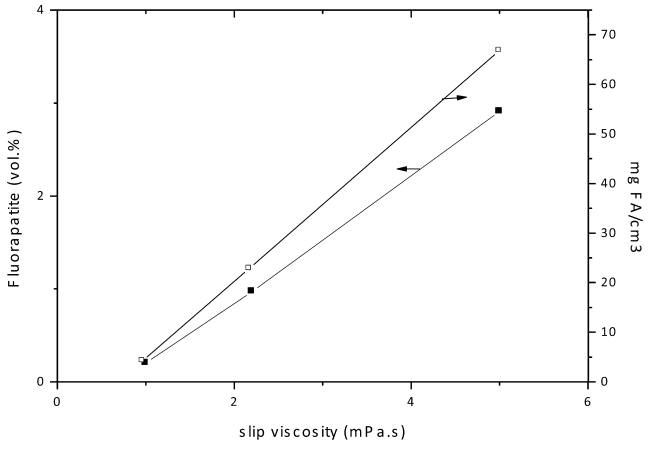

FIGURE 4 Volume percent of the scaffold porosity occupied by FA and amount of FA introduced into the scaffolds per cm^3 as a function of the slip viscosity

uncoated and coated scaffolds with slips of 5.0 mPa.s viscosity, respectively (Figure 5B).

Figure 6A, B shows the volume percent of the scaffold porosity occupied by FA and the amount of FA introduced into the scaffold per cm^3, respectively, for the different dip coating slip viscosities as a function of the immersion time. The vol% of FA and the mg FA/cm^3 of ZrO_2 scaffolds coated with slips with very low viscosity hardly changed with prolonged immersion time up to 10 seconds and remained below 0.5 vol% and 5 mg FA/cm^3. In contrast, these values gradually increased with increasing immersion time for 2.2 and 5.0 mPa.s slip viscosities.

The coating with slips having very low viscosity did not lead to a continous FA film at all the immersion times studied, therefore the pore size distribution of the ZrO_2 scaffolds was not altered. The pore size distributions of the ZrO_2 scaffolds after coating with slips of 2.2 and 5.0 mPa.s viscosity for different immersion times are, respectively, shown in Figure 7A,B. For ZrO_2 scaffolds coated with slips of 2.2 mPa.s viscosity, the increase in the immersion time from 2 to 10 seconds produced a displacement of the more frequent pore size from 360-380 to 280-300 μm, whereas a greater displacement from 240-260 to 120-140 μm occurred after coating with slips of 5.0 mPa.s viscosity. This was in agreement with the higher occupation rate of the scaffold porosity by FA when the dip coating slip of 5.0 mPa.s viscosity was used (Figure 6). It was expected that the large amount of FA introduced in the scaffolds coated with slips of 5.0 mPa.s viscosity at all the immersion times would certainly decrease its biological activity by reducing the pore volume and the pore size. Therefore, the biological studies were performed on ZrO_2 scaffolds coated with slips of 2.2 mPa.s for 2 seconds and compared with uncoated scaffolds.

3.2 | Biological studies

The osteogenic cell response to the uncoated and FA coated ZrO_2 scaffolds was assessed in terms of cell spreading and

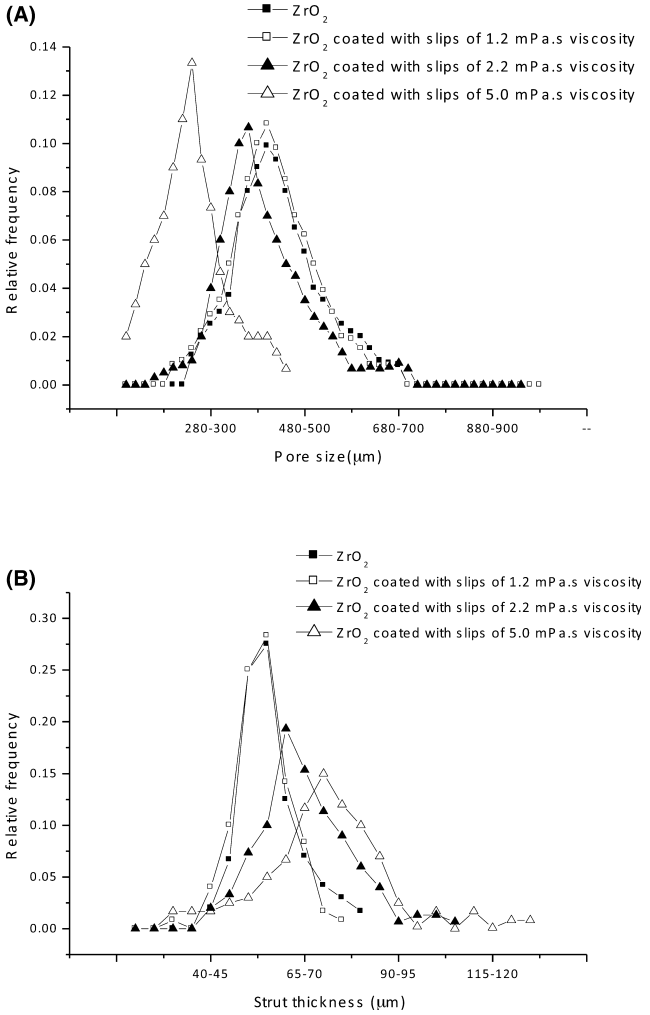

FIGURE 5 Macropore size distribution (A) and strut thickness distribution (B) of ZrO_2 scaffolds before and after coating with slips of 1.2, 2.2, and 5.0 mPa.s viscosity for 2 s

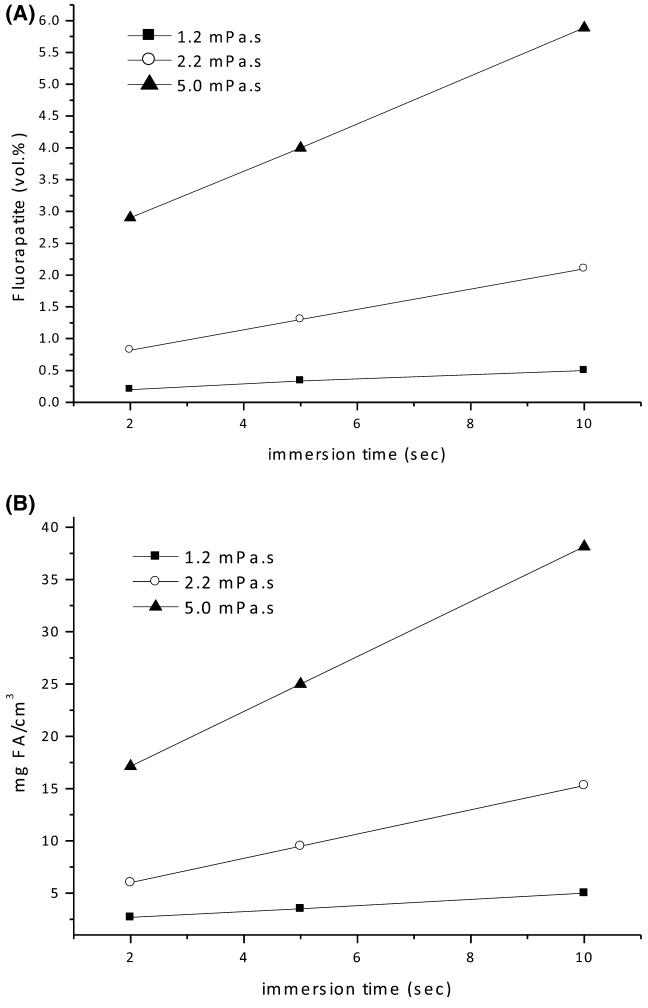

FIGURE 6 Volume percent of the scaffold porosity occupied by FA (A) and amount of FA introduced into the scaffold per cm^3 (B), for the different dip coating slip viscosities as a function of the immersion time

survival. The results showed that the pre-osteoblastic MC3T3-E1 cells were adhered, spread and sparsely distributed on both scaffold surfaces at 2 days of culture, showing either polygonal or elongated shapes (Figure 8). At 7 days of culture, the MTT analysis showed that a layer of viable MC3T3-E1 cells or BMSC was readily apparent throughout the upper (seeded side) surface of the uncoated and FA coated ZrO_2 scaffold structures (Figure 9). The macroscopic observation of more viable cells in BMSC cultures compared with MC3T3-E1 ones was corroborated by the absorbance readings obtained spectrophotometrically (Figure 9), indicating that spreading-dependent cell proliferation was more pronounced for the undifferentiated BMSC cultures.

4 | DISCUSSION

The rheological behavior of FA suspensions can be affected by the FA solubility in aqueous solution. We have previously investigated[18] the FA surface reactivity in an aqueous solution having different pH values with a concentration of ammonium polyacrylate, as a function of time. Our results demonstrated that the FA dissolution rate via Ca^{++}/H^+ exchange markedly decreased in weakly alkaline (pH 9) conditions, avoiding both an increase in the ionic strength of the suspension and a change in the FA surface composition. Therefore, the aqueous colloidal processing of the FA dip coating suspensions with NH_4PA was performed at pH 9. In the same work[18] we have studied the rheological behavior of aqueous FA slips stabilized with NH_4PA, the isoelectric point (IEP) of the FA powder was at about pH 6; the FA exhibited a negative surface charge at pH > 6 and a positively one at pH values lower than the IEP. The fluorapatite surfaces consisted of $\equiv CaOH^+$ groups below the isoelectric point, the $\equiv CaOH^+$ concentration decreased with increasing pH and at alkaline pH values $\equiv PO_4^{-3}$ groups or protonated phosphate groups

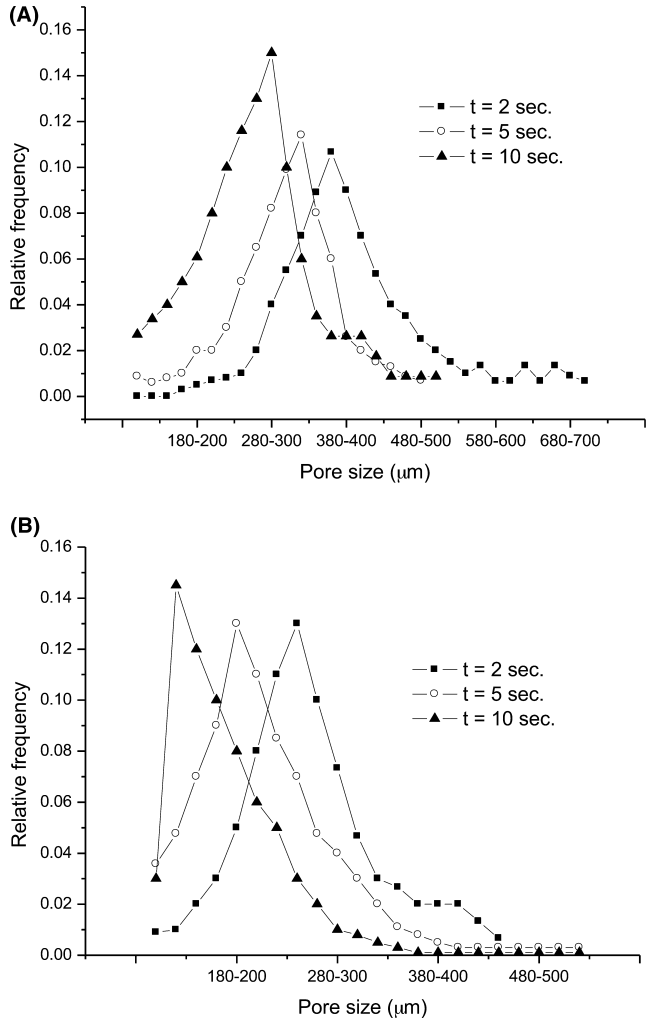

FIGURE 7 Macropore size distribution of ZrO_2 scaffolds after coating with slips of 2.2 mPa.s (A) and 5.0 mPa.s viscosity (B), for different immersion times

($\equiv HPO_4^{-2}$, $\equiv H_2PO_4^{-1}$) predominated. Albano and Garrido[18] observed that the addition of NH_4PA shifted the IEP of FA toward a lower pH value of 5. The ammonium polyacrylate dissociates according to the following reaction:

$$RCOONH_4 \rightarrow RCOO^- + NH_4 \quad (5)$$

Since the degree of dissociation was nearly 1 at pH values ≥8.5,[10] the polymer charge is negative at those pH values. During the aqueous colloidal processing of the FA powder with 0.6 wt% NH_4PA, the pH of the suspension was adjusted at 9. At this pH, the $RCOO^-$ groups of the deflocculant were specifically adsorbed on the FA powder surface. The adsorption of the negatively charged polyelectrolyte increases the negative surface charge of the FA powder and consequently the electrostatic repulsion between particles, thereby low viscosity values were achieved (Figure 1).

As the solid loading increased from 5 to 20 wt% the hydrodynamic and particle interactions increased, thereby increasing the FA slip viscosity (Figure 1). Stábile et al[19] have recently determined that the degree of slip dispersion of a ceramic powder at low solid loading (20 wt%) was nearly the same with and without PVA; thus, the PVA did not affect the dispersion properties of the FA powder.

The ZrO_2 scaffold exhibited a well-developed interconnected macropore structure (Figure 2); the scaffold total porosity was nearly almost open or interconnected, only a few pores were blocked or closed. The achievement of a highly open porous structure is beneficial for more effective penetration of the fluorapatite coating and ensures migration of cells and tissue formation into the ZrO_2 scaffold structure as suggested by D'Angelo et al.[20]

Calambás Pulgarin et al[21] determined the particle size distribution curve of the ZrO_2 powder. The more frequent particle diameters were 0.37 and 0.65 μm; a lesser volume of finer particles (<0.40 μm) and a greater volume of particles with diameters in the range of 0.40-1.05 μm were observed. The zeta potential as a function of pH curves for aqueous ZrO_2 suspensions with and without NH_4PA were previously studied.[22] The high negative zeta potential of the ZrO_2 suspensions with 0.11 wt% NH_4PA at pH 9 (-63 mV) produced well dispersed suspensions. During centrifugation of the polyurethane foams immersed in the ZrO_2 slurry, the penetration of coarse (0.40-1.05 μm) ZrO_2 particles into the foams would preferentially occurred. As a consequence residual microporosity could be expected in the ZrO_2 scaffolds after sintering. Soubelet et al[23] reported that ZrO_2 slip cast compacts reached ~98% of the theoretical density at 1500°C, this result indicated that full densification of ZrO_2 was not achieved.

The coating of the ZrO_2 scaffolds with the lowest viscosity FA slip produced an inhomogeneous film along the strut surfaces (Figure 2B). The amount of FA introduced into the ZrO_2 scaffold and the decrease in the scaffold porosity after the coating procedure were almost negligible (Figure 4), indicating a non-uniform distribution of the coating in the structure. The very low viscosity of the aqueous 5 wt% slip (Figure 1) caused a rapid flow after infiltration and avoided an homogeneous coating; thus, this slurry did not present enough viscosity to remain in the ZrO_2 scaffold during drying. Rambo et al[24] revealed that an adequate slip to produce a coating must be fluid enough to penetrate into the structure and also presents enough viscosity to remain in it. As a consequence, the 5 wt% dip coating slurry did not lead to a continuous FA film along the strut network and the macropores remained uncoated.

The well-dispersed FA slip with 2.2 mPa.s viscosity enabled a greater incorporation of FA into the scaffold (Figure 4), resulting in a coating uniformly distributed along the strut surfaces (Figure 2C) and inside the

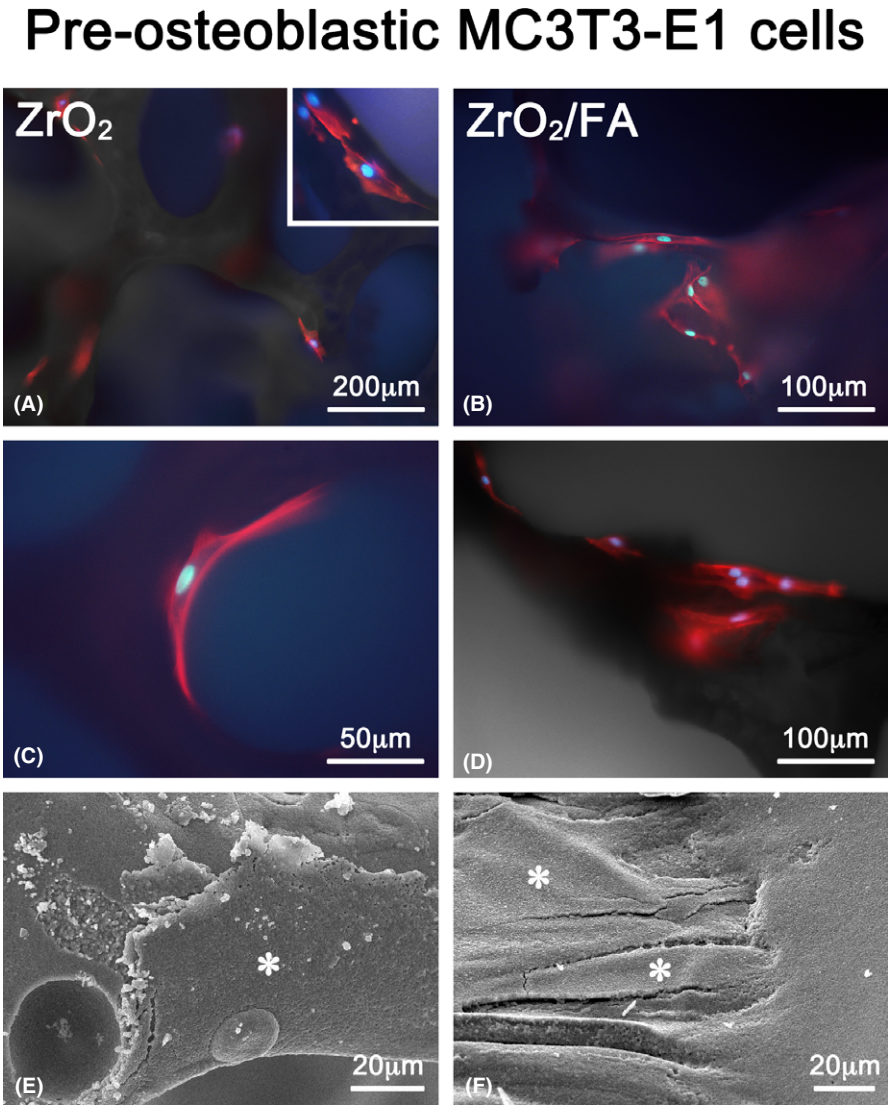

FIGURE 8 Epifluorescence microscopy (A-D) and SEM images (E-F) of pre-osteoblastic MC3T3-E1 cells grown on uncoated (A, C, E) and coated (B, D, F) ZrO_2 scaffolds at 2 days of culture. (A-D) Red fluorescence indicates actin cytoskeleton (labelled with Alexa Fluor 594-conjugated phalloidin) and blue fluorescence indicates cell nuclei (labelled with DAPI). The upper surface of the scaffold structure (seeded side) exhibited adhered and spread cells with either polygonal or elongated shapes. (E, F) SEM images confirmed the epifluorescence observation, and revealed that the cells were well flattened on both scaffold surfaces (asterisks)

macropores forming a thin FA layer (Figure 3A); the thickness of the adhered layer was about 6-20 μm. This thin FA layer did not change the polygonal shape of the ZrO_2 scaffold macropores (Figure 2C). It was possible to observe (Figure 3A) that the well-dispersed FA slip was able to infiltrate and filled small pores and surface defects of the ZrO_2 scaffold structure derived from the sintering process.

The higher viscosity value of the 20 wt% FA slip with respect to that of 10 wt% (Figure 1) formed an homogeneous coating along the strut network and produced thicker adhered layers (30-100 μm) inside the pores (Figures 2D and 3B). The pores with small sizes were completed closed by FA, whereas the ones with large sizes were partially blocked (Figure 2D). Two mechanisms govern the formation of a layer on a porous body during dip coating[25]; the first mechanism is known as liquid entrainment and the second one is a slip casting phenomenon. The liquid entrainment which occurs at the initial stage leaves a thin adhered layer, the thickness of this layer, h, can be expressed as[25]:

$$h = 0.94\left(\frac{\gamma}{\delta g}\right)^{1/2} \mathrm{Ca}^{2/3} \tag{6}$$

Ca is the capillary number given by:

$$\mathrm{Ca} = \frac{\mu V}{\gamma} \tag{7}$$

where γ is the surface tension, δ is the slurry density, g is the gravity acceleration, μ is the slurry viscosity and V is the withdrawal velocity.

Assuming similar slurry densities for the FA slips, the film thickness given by Equations (6) and (7) is dependent on both the withdrawal velocity of the specimen and the suspension viscosity. As the experiments of dip coating with the different FA slips were performed using identical withdrawal velocity, the thickness of the layer was directly

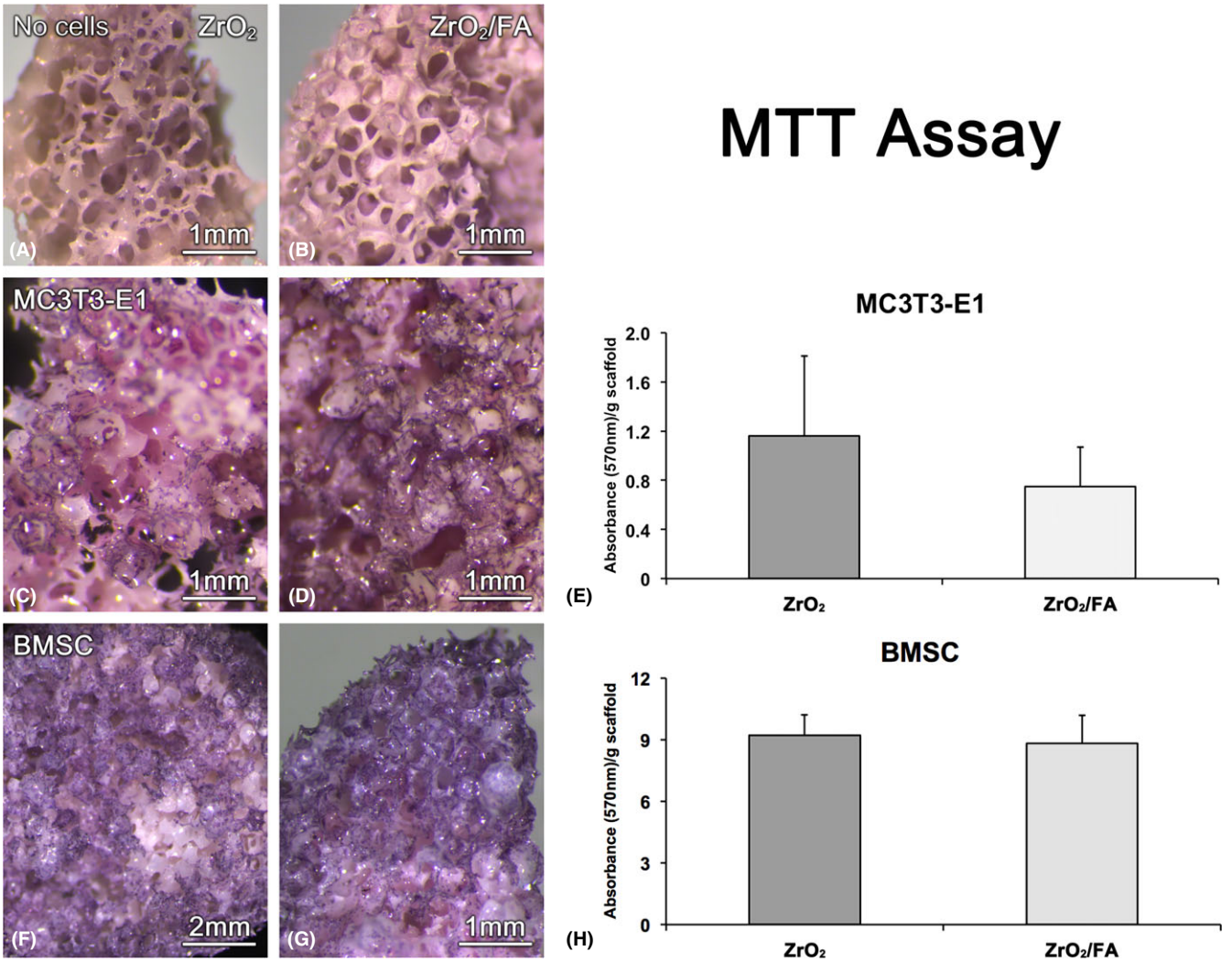

FIGURE 9 MTT assay of pre-osteoblastic MC3T3-E1 and BMSC cultures grown on uncoated and coated ZrO_2 scaffolds at 7 days of culture. The ZrO_2 and ZrO_2/FA scaffolds with no cells are shown in A and B images. No significant differences in terms of cell viability between uncoated and coated ZrO_2 scaffolds were observed for MC3T3-E1(C, D, E) and BMSC (F, G, H) cultures. Formazan-stained areas (purplish spots) were more pronounced for the BMSC cultures (compare F and G with C and D, respectively)

related with the slurry viscosity. The greater thickness of the layer produced using the 20 wt% FA slip was attributed to its higher viscosity and its effect on the liquid entrainment mechanism. Thus, as the FA slip viscosity increased from 2.2 to 5 mPa.s a greater thickness of the film adhered was measured.

For the 20 wt% dip coating slurry a significant volume percent of the ZrO_2 scaffold porosity was occupied by the FA adhered layer (Figure 4), producing an important reduction in the scaffold pores volume and a change in the pores shape from polygonal (in the uncoated scaffold) to round or irregular (in the scaffold coated with slips of 5.0 mPa.s viscosity; Figure 2).

The low amount of FA introduced into the scaffold after coating with FA slips having the lowest viscosity value resulted in an inhomogeneous coating which did not reduce the porosity or increased the strut thickness of the original ZrO_2 scaffold structure (Figure 5A,B). A reduction in porosity of 1vol% and a slightly displacement of the more frequent pore size from 400-420 to 360-380 μm (Figures 4 and 5) were achieved after coating the ZrO_2 scaffolds with slips of 2.2 mPa.s viscosity. In contrast, the coating with slips of 5.0 mPa.s viscosity produced a partial blocking of macropores, affecting the whole porous structure of the ZrO_2 scaffolds.

A linear relation between the vol% of FA and the immersion time was found for the different dip coating slip viscosities (Figure 6A). As it was previously mentioned, the formation of a layer on the internal surface of the porous is governed by liquid entrainment at the initial stage and slip casting for longer immersion times. In the slip casting process the driving force for the liquid flow is the

capillary suction pressure caused by the microporosity of the scaffolds. A linear relationship between the layer thickness squared and the immersion time have been reported[26,27]; as a consequence, the volume percent of the scaffold porosity occupied by FA and the amount of FA introduced into the scaffold per cm^3 increased with increasing immersion time for the different dip coating slip viscosities (Figure 6A, B).

A comparison of the line slopes indicated that the rate at which the scaffold porosity was occupied by FA increased with increasing the slip viscosity up to 5.0 mPa.s. The higher occupation rate of the scaffold porosity by FA with increasing the slip viscosity produced a greater displacement of the more frequent pore size to lower sizes (Figure 7A,B). Some of the macropores became rounded with increasing the immersion time from 2 to 10 seconds after coating with slips of 2.2 mPa.s, in accordance with the greater amount of FA introduced (Figures 2C, E and 6). For dip coating slips having 5.0 mPa.s viscosity, the partial blocking of pores by the FA coating occurred to a greater extent in scaffolds infiltrated 10 seconds compared with those infiltrated 2 seconds, as shown in Figures 2D, F and 3B, C. Figure 3D shows the microstructure of the FA coating layer after infiltration for 10 seconds with slips having 5.0 mPa.s viscosity; less densification, thus, an increase in the layer porosity with increasing its thickness could be observed. Besides, there was a close relation between the density and the volumetric shrinkage of the layer upon sintering, as the density of the layer decreased (or the porosity increased) a higher volumetric shrinkage could be expected. The different sintering shrinkage behaviour within the layer formed inside the macropores might produce microcracks as observed in Figure 2F.

As previously demonstrated,[28] the cellular response in terms of adhesion, proliferation and mineralization on ZrO_2 depends on its chemical composition and on the physicochemical surface properties (topography, wettability), as well as porous microstructure characteristics. In this work, the in vitro assays demonstrated that the FA coating of ZrO_2 scaffold yielded a favorable combination of surface and microstructure properties to support MC3T3-E1 and BMSC spreading and survival over a short-term culture period. Considering that BMSC and osteoblast-committed cells migrate into the scaffold during the bone healing process in vivo, further studies are needed to evaluate the impact of the FA coating of ZrO_2 scaffolds on the osteogenic potential of both cell sources. Nevertheless, the dip coating process provided a well-adhered FA coating on ZrO_2 surface with favorable biological behaviour (uniform morphology and cell spreading) and similar biocompatibility to that of uncoated ZrO_2 structure.

5 | CONCLUSIONS

Three dimensional, highly porous, ZrO_2 scaffolds coated by fluorapatite were fabricated. The FA coating was achieved by dipping the ZrO_2 scaffold into stabilized aqueous FA slips having viscosity values ≤5.0 mPa.s. The results demonstrated that the slip viscosity of the suspensions and the immersion time greatly affected the amount of FA introduced into the scaffold and the resultant coated scaffold structure. The dip coating FA slip with very low viscosity did not lead to a continuous film along the strut network and the macropores remained uncoated. The slips with the highest viscosity value (5.0 mPa.s) produced a partial blocking of macropores, which increased with increasing the immersion time. The porous structure obtained with slips of 2.2 mPa.s viscosity for 2 seconds, attained a reduction in porosity of 1 vol% and a more frequent pore size in the range 360-380 μm. The continuous film distributed along the strut surfaces and the FA layer inside the macropores supported spreading and survival of either pre-osteoblastic MC3T3-E1 cells or BMSC over a short-term culture period. Although similar cell viability for both cell cultures grown on uncoated and FA coated ZrO_2 structures was detected, the MTT values were significantly higher for BMSC at 7 days of culture. Moreover, the biological evaluation indicated that the surface properties of the FA coating did not affect the initial osteogenic cell biocompatibility of ZrO_2 scaffolds.

ACKNOWLEDGMENT

This work was financially supported by FAPESP-CONICET (2012/50949-4) and CONICET (PIP 0454).

ORCID

María Albano http://orcid.org/0000-0002-5235-0032

REFERENCES

1. Weiner S, Wagner HD. The material bone: structure-mechanical function relations. *Annu Rev Mater Sci*. 1998;28:271-298.
2. Vallet-Regí M, González-Calbet JM. Calcium phosphates as substitution of bone tissues. *Prog Solid State Chem*. 2004;32:1-31.
3. Dorozhkin SV. Nanodimensional and nanocrystallineapatites and other calcium orthophosphates in biomedical engineering, biology and medicine. *Materials*. 2009;2:1975-2045.
4. Suchanek W, Yoshimura M. Processing and properties of hydroxyapatite-based biomaterials for use as hard tissue replacement implants. *J Mater Res*. 1998;13:94-117.
5. Cheng K, Weng W, Han G, et al. The effect of trtriethanolamine on the formation of sol-gel derived fluorapatite/hydroxyapatite solid solution. *Mater Chem Phys*. 2003;78:767-771.

6. Cheng K, Shen G, Weng W, et al. Synthesis of hydroxyapatite/fluorapatite solid solution by a sol-gel method. *Mater Lett*. 2001;51:37-41.
7. Kelly JR, Denry I. Stabilized zirconia as a structural ceramic: an overview. *Dent Mater*. 2008;24:289-298.
8. Piconi C, Maccauro G. Zirconia as a ceramic biomaterial. *Biomaterials*. 1999;20:1-25.
9. Chen QZ, Thompson ID, Boccaccini AR. 45S5 Bioglass-derived glass-ceramic scaffolds for bone tissue engineering. *Biomaterials*. 2006;27:2414-2425.
10. Cesarano J, Aksay IA. Processing of highly concentrated aqueous α-alumina suspensions stabilized with polyelectrolytes. *J Am Ceram Soc*. 1988;71:1062-1067.
11. Guldberg-Pedersen H, Bergström L. Stabilizing ceramic suspensions using anionic polyelectrolytes: adsorption kinetics and interparticle forces. *Acta Mater*. 2000;48:4563-4570.
12. Malmström J, Adolfsson E, Emanuelsson L, et al. Bone ingrowth in zirconia and hydroxyapatite scaffolds with identical macroporosity. *J Mater Sci Mater Med*. 2008;19:2983-2992.
13. Kim HW, Shin SY, Kim HE, et al. Bone formation on the apatite-coated zirconia porous scaffolds within a rabbit calvarial defect. *J Biomater Appl*. 2008;22:485-504.
14. Malmström J, Slotte C, Adolfsson E, et al. Bone response to free form-fabricated hydroxyapatite and zirconia scaffolds: a histological study in the human maxilla. *Clin Oral Implants Res*. 2009;20:379-385.
15. Maniatopoulos C, Sodek J, Melcher AH. Bone formation in vitro by stromal cells obtained from bone marrow of young adult rats. *Cell Tissue Res*. 1988;254:317-330.
16. Albano MP, Calambás Pulgarin HL, Garrido LB, et al. Effect of ZrO_2 content on ageing resistance and osteogenic cell differentiation of ZrO_2-Al_2O_3 composite. *Ceram Int*. 2016;42:11363-11372.
17. Pereira KK, Alves OC, Novaes AB Jr, et al. Progression of osteogenic cell cultures grown on microtopographic titanium coated with calcium phosphate and functionalized with a type I collagen-derived peptide. *J Periodontol*. 2013;84:1199-1210.
18. Albano MP, Garrido LB. Processing of concentrated aqueous fluorapatite suspensions by slip casting. *J Mater Sci*. 2011;46:5117-5128.
19. Stábile FM, Albano MP, Garrido LB, et al. Processing of ZrO_2 scaffolds coated by glass-ceramic derived from 45S5 bioglass. *Ceram Int*. 2016;42:4507-4516.
20. D'Angelo C, Ortona A, Colombo P. Finite element analysis of reticulated ceramics under compression. *Acta Mater*. 2012;60:6692-6702.
21. Calambás Pulgarin HL, Garrido LB, Albano MP. Comparison of different zirconia powders for slip casting of alumina-zirconia ceramics. *Adv Appl Ceram*. 2013;112:39-45.
22. León B, Albano MP, Stábile FM, Garrido LB. Processing of concentrated aqueous zirconia-bioglass slips by slip casting. *Ceram Silikaty*. 2017;61:1-10.
23. Soubelet CG, Albano MP, Conconi MS. Sintering, microstructure and hardness of Y-TZP-64S bioglass ceramics. *Ceram Int*. 2018;44:4868-4874.
24. Rambo CR, De Sousa E, Novaes de Oliveira AP, et al. Processing of cellular glass ceramics. *J Am Ceram Soc*. 2006;89:3373-3378.
25. Pontin MG, Lange FF, Sánchez-Herencia AJ, et al. Effect of unfired tape porosity on surface film formation by dip coating. *J Am Ceram Soc*. 2005;88:2945-2948.
26. Gu Y, Meng G. A model for ceramic membrane formation by dip-coating. *J Eur Ceram Soc*. 1999;19:1961-1966.
27. Albano MP, Garrido LB, Teixeira LN, et al. Comparison of different fluorapatite dip coated layers on porous zirconia tapes. *Ceram Int*. 2014;40:12509-12517.
28. Soon G, Pingguan-Murphy B, Lai KW, et al. Review of zirconia-based bioceramic: surface modification and cellular response. *Ceram Int*. 2016;42:12543-12555.

How to cite this article: León B, Albano M, Garrido L, Ferraz E, Rosa A, Tambasco de Oliveira P. Processing, structural, and biological evaluations of zirconia scaffolds coated by fluorapatite. *Int J Appl Ceram Technol*. 2018;00:1-12. https://doi.org/10.1111/ijac.12904